TOWARDS 3D MAPPING OF FORESTS: A COMPARATIVE STUDY WITH FIRST/LAST PULSE AND FULL WAVEFORM LIDAR DATA

J. Reitberger [a], Cl. Schnörr [b], M. Heurich [c], P. Krzystek [a, *], U. Stilla [d]

[a] Dept. of Geoinformatics, University of Applied Sciences Muenchen, 80333 Munich, Germany-
(josef.reitberger, krzystek)@hm.edu
[b] Dept. of Computer Science and Mathematics, University of Applied Sciences Muenchen, 80335 Munich, Germany-
schnoerr@cs.hm.edu
[c] Dept. for Research and Documentation, Bavarian Forest National Park, 94481 Grafenau, Germany -
marco.heurich@npv-bw.bayern.de
[d] Photogrammetry and Remote Sensing, Technische Universitaet Muenchen, 80290 Munich, Germany-
stilla@tum.de

Commission VIII, ThS-21

KEY WORDS: LIDAR, Analysis, Segmentation, Forestry, Vegetation

ABSTRACT:

This paper highlights several approaches to segment and reconstruct trees from LIDAR data and compares the results acquired both from first/last pulse and full waveform data. In a first step, we set up a conventional watershed based segmentation procedure, which robustly interpolates the CHM from the LIDAR data and finds possible stem positions of the tallest trees in the segments calculated from the local maxima of the CHM. Secondly, we combine this segmentation approach with a special stem detection method. Stem positions in the segments of the watershed segmentation are detected by hierarchically clustering points below the crown base height and reconstructing the stems with a robust RANSAC-based adjustment of the stem points. Finally, we implement a new 3D segmentation of single trees using the normalized cut method. This tackles the problem of how to segment small trees below the CHM. Experiments were conducted in the Bavarian Forest National Park with conventional first/last pulse data and full waveform LIDAR data. The first/last pulse data were collected in a flight with the Falcon II system from TopoSys in a leaf-on situation at a point density of 10 points/m². Full waveform data were captured with the Riegl LMS Q-560 system at a point density of 25 points/m² (leaf-off and leaf-on) and at a point density of 10 points/m² (leaf-on). The study results prove that the new 3D segmentation approach is capable of detecting small trees in the lower forest layer. So far, this has been practically impossible when tree segmentation techniques based on the CHM were applied to LIDAR data. Compared to the standard watershed segmentation procedure, the combination of the stem detection method and the normalized cut segmentation leads to the best segmentation results and is superior in the best case by 12%. Moreover, the experiments show clearly that the usage of full waveform data is superior to first/last pulse data.

1. INTRODUCTION

The development of new approaches to forest inventory utilising remote sensing data has been an important research issue in the past. Beside area based methods, techniques for single tree extraction from LIDAR data have been investigated for mapping forests at the tree level and for identifying important parameters, such as tree height, crown size, crown base height, and tree species. Most of the techniques reconstruct - at least locally - the canopy height model (CHM) using only the LIDAR points on the canopy surface and find tree positions from the local maxima. Methods presented by Hyyppä et al. (2001), Solberg et al. (2006), and Brandtberg (2007) represent such approaches. Typically, the detection rate of single trees is limited due to unavoidable smoothing effects in the interpolated surface. The main drawback is that trees and young regeneration in the middle and lower forest layer are invisible from the CHM surface and, hence, cannot be detected at all. Recent advances in LIDAR technology have generated new full waveform scanners that provide a higher spatial point density as well as additional information on the reflecting characteristics

of the internal forest structure. Such scanners have been available for about three years and have been used in research by several groups. Wagner et al. (2006) focused on the calibration issue and the decomposition of full waveform data with a series of Gaussians. Also, Wagner et al. (2006) showed that different types of vegetation, such as trees and bushes can be separated using the cross section calculated from the waveforms. Jutzi and Stilla (2006) fit Gaussians to the surface response that is obtained by measurement of the individual emitted waveform and a corresponding deconvolution of the received waveform. Recently, Kirchhof et al. (2008) presented a method to improve the reconstruction of buildings partly occluded by vegetation by pre-segmenting reflections from the vegetation using the surface response. Reitberger et al. (2008a) also showed the decomposition of waveforms by fitting Gaussians to the waveform. Compared to conventional first/last pulse data, an increase in the point density by a factor of 3 could be verified. The classification of coniferous and deciduous trees is successfully demonstrated using salient

---

* Corresponding author.

features calculated from the pulse width and the intensity of the decomposed waveform.

Obviously, full waveform data render possible new approaches to reconstruct and classify objects, such as trees. However, an important question that still needs to be resolved is: how much do full waveform data really improve forest inventory methods compared to conventional first/last pulse data? More precisely, it will be certainly interesting to find out whether new extraction methods for single trees can be developed that take advantage of full waveform data and improve the detection rate significantly.

Thus, the objective of this paper is (i) to shortly highlight new segmentation methods that extract single trees using full waveform LIDAR data, (ii) to present the results of the methods when applied to first/last pulse data and full waveform data acquired in the same area in leaf-on and leaf-off situations at different point densities, and (iii) to compare the methods with respect to the success rate.

The paper is divided into five sections. Section 2 highlights three different segmentation methods. Section 3 shows the results that were obtained from conventional first/last pulse data (TopoSys Falcon II) and full waveform data (Riegl LMS-Q560) acquired in the Bavarian Forest National Park. Finally, the results are discussed with conclusions in sections 4 and 5.

2. METHODOLOGY

2.1 Pre-processing of LIDAR data

We assume a point cloud in a region of interest (ROI) represented by $X_i^T = (x_i, y_i, z_i, W_i, I_i)(i = 1,..., N_{ROI})$ LIDAR points that result from reflections of the laser beam at the positions (x_i, y_i, z_i). In the case of a full waveform scanner, waveform decomposition provides the pulse width W_i and the intensity I_i as attributes (Jutzi and Stilla, 2005; Reitberger et al., 2008a). In comparison, conventional LIDAR systems provide only the coordinates of the reflections (x_i, y_i, z_i) and – in many cases – also the intensity. Since, in general, it is unknown how the intensity value is recorded in the conventional first/last pulse LIDAR systems, this parameter has not yet been considered of practical importance. The advantage of full waveform LIDAR data is that, basically, each reflection can be detected by the waveform decomposition. This is remarkable since conventional LIDAR systems – recording at most 5 reflections – have a dead zone of about 3 m, which make these systems effectively blind after a single reflection. The calibration of the values W_i and I_i is achieved by using the pulse width W^e and the intensity I^e of the emitted Gaussian pulse. Additionally, the intensity is corrected with respect to the run length s_m of the laser beam and a nominal distance s_0 with

$$W_m^c = W_m / W^e \tag{1}$$

$$I_m^c = (I_m \cdot s_m^n) / (I^e \cdot s_0^n) \tag{2}$$

assuming a target size larger or equal to the footprint (Wagner et al., 2006). The factor n amounts theoretically to the value 2. In practice, however, it might deviate depending on the LIDAR system.

2.2 Watershed segmentation

A first crude segmentation of the tree crowns is calculated from a CHM by the watershed algorithm (Vincent and Soille, 1991). The CHM is interpolated by means of least squares from the LIDAR points best representing the tree shapes (Reitberger et al., 2008a). The local maxima of the watershed segments define possible tree positions $(X_{stem\ i}^{CHM}, Y_{stem\ i}^{CHM})(i = 1,..., N_{seg})$ (Fig. 1). Note that the interpolation process smoothes the CHM surface considerably in order to avoid over-segmentation. Thus, neighbouring trees are often not separated and, instead, form a tree group made up of single trees. Moreover, smaller trees in the intermediate and lower height levels cannot be recognised since they are not visible in the CHM.
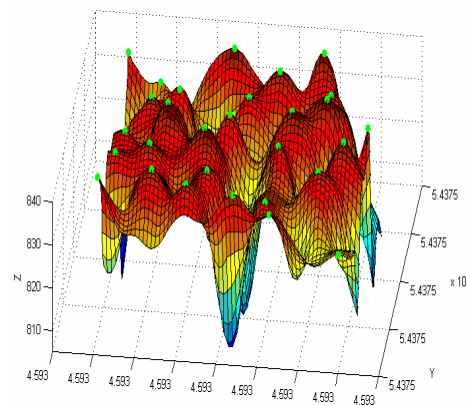

Figure 1. Reconstructed CHM with local maxima as tree tops

2.3 Stem detection

The key idea of the stem detection is to separate neighbouring trees that have been combined to form a tree group and to improve the accuracy of the tree positions calculated from the local maxima. The approach is motivated by the observation that in case of full waveform data the stems of trees are very often clearly visible. The method works in a 3-step algorithm. First, it isolates points of the stem area from the crown points using an appropriate crown base height (Fig. 2a). Second, possible stem points are found by hierarchically clustering of these points using their horizontal distances. Third, the stem position is estimated with a robust RANSAC-based adjustment of the stem points (Reitberger et al., 2007). Note that several stems can be found within a tree segment. The figures 2b and 2c show a group of beech trees that are merged to one segment by the watershed algorithm. The stem detection method was able to identify the four stems that had been verified in the reference data. Thus, this approach improves the detection rate of single trees in the intermediate and upper tree level and the accuracy of the tree positions originally provided by the watershed segmentation. However, the crown points belonging to the original segment are not separated with respect to the detected stems. The stem positions $(X_{stem\ i}^{StDet}, Y_{stem\ i}^{StDet})(i = 1,..., N_{StDet})$ provided by the stem detection are used later on in the 3D segmentation.
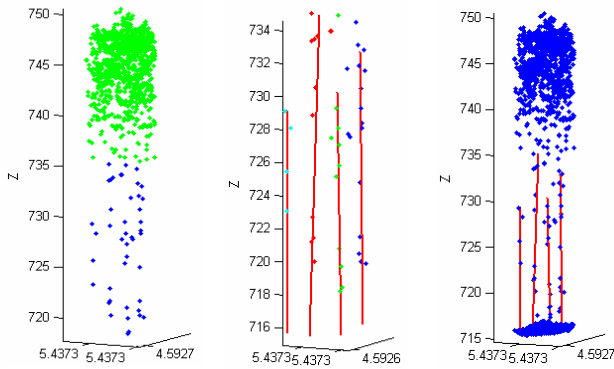
Figure 2. A group of beeches where a) crown and stem points are separated and b) and c) stems are reconstructed with RANSAC

2.4 Normalized cut segmentation

The stem detection works perfectly if there are enough stem reflections and if the stem area can be reliably separated from the crown points by the crown base height. It fails of course when young regeneration and small trees are located below tall trees. In order to tackle this problem, we have set up a true 3D segmentation of single trees using the normalized cut method known from image segmentation (Shi and Malik, 2000).
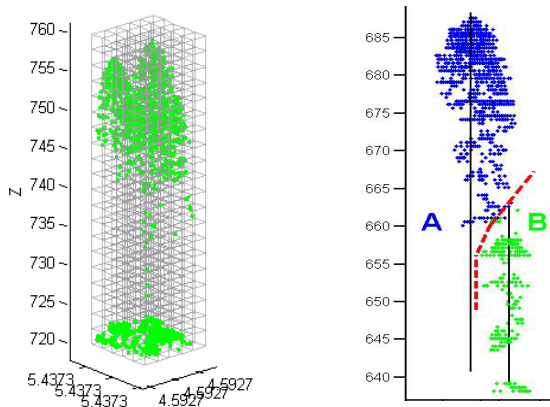

Figure 3a. Subdivision of ROI into a voxel structure

Figure 3b. Division of voxels into two tree segments *A* and *B*.

The normalized cut segmentation divides a graph *G* formed by the voxels (Fig. 3a) into disjoint voxel segments *A* and *B* (Fig. 3b) by maximising the similarity of the segment members and minimising the similarity between the segments *A* and *B*. The corresponding cost function is

$$NCut(A,B) = \frac{Cut(A,B)}{Assoc(A,V)} + \frac{Cut(A,B)}{Assoc(B,V)} \qquad (3)$$

with $Cut(A,B) = \sum_{i \varepsilon A, j \varepsilon B} w_{ij}$ as the total sum of weights between

the segments *A* and *B* and $Assoc(A,V) = \sum_{i \varepsilon A, j \varepsilon V} w_{ij}$ representing

the sum of the weights of all edges ending in the segment *A*. The weights w_{ij} between two voxels are basically a function of the LIDAR point distribution and features calculated from the pulse width W_i and the intensity I_i. They define the similarity between the voxels. The minimisation of *NCut(A,B)* is solved by the corresponding generalised eigenvalue problem (Reitberger et al., 2008b).
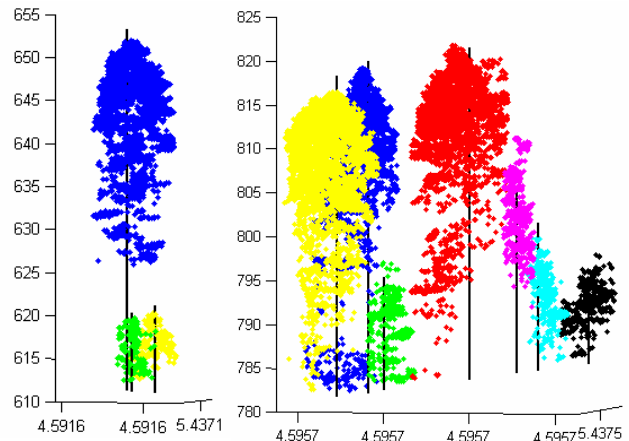

Figure 4. Examples of normalized cut segmentation

The approach can use auxiliary data, such as for instance, information on the local maxima of a CHM $(X^{CHM}_{stem\ i}, Y^{CHM}_{stem\ i})(i=1,...,N_{seg})$, in order to weight the similarity between the voxels below the CHM maxima. Also, the results of the stem detection $(X^{StDet}_{stem\ i}, Y^{StDet}_{stem\ i})(i=1,...,N_{StDet})$ can be introduced to provide special weights for similarity between the voxels. The figure 4 shows complex situations where the normalized cut segmentation works excellently and where the watershed segmentation and stem detection approaches fail.

3. EXPERIMENTS

3.1 Material

Experiments were conducted in the Bavarian Forest National Park (49° 3' 19" N, 13° 12' 9" E). 18 sample plots with an area size between 1000 m² and 3600 m² were selected in the mixed mountain forests. Reference data for all trees with DBH larger than 10 cm were collected for 688 Norway spruce (*Picea abies*), 812 European beeche (*Fagus sylvatica*), 70 fir (*Abies alba*), 71 Sycamore maple (*Acer pseudoplatanus*), 21 Norway maple (*Acer platanoides*) and 2 lime trees (*Tilia europaea*). Tree parameters, such as DBH, total tree height, stem position, and tree species were measured and determined by GPS, tacheometry, and the 'Vertex III' system. First/last pulse data were recorded by TopoSys with the Falcon II system. Full waveform data were collected by Milan Flug GmbH using the Riegl LMS-Q560 system. Table 1 contains details on the point density, leaf-on and leaf-off conditions during the flights and the footprint size. The term point density is referring to the nominal value influenced by the PRF, flying height, flying speed and strip overlap. These data sets allow the comparison of conventional and full waveform systems, which were flown in the same area. However, the data set IV is only available for 12 reference plots, referred to as 'Area E'. This has to be considered when comparing results of other data sets with this

data set. Naturally, the reference data were updated for the individual flying dates. Reference trees are plotted in the figures 3, 4, 6 and 7 as black vertical lines.

Time of flight	Sept. '02	May '06	May '07	May '07
Data set	I	II	III	IV
Foliage	Leaf-on	Leaf-off	Leaf-on	Leaf-on
Scanner	TopoSys Falcon II	Riegl LMS-Q560	Riegl LMS-Q560	Riegl LMS-Q560
Pts/m^2	10	25	25	10
FOV [deg]	14.3	45	60	60
HAAT [m]	850	400	400	500
Footprint [cm]	85	20	20	25
Ref. plots	all	all	all	Area E

Table 1. Different ALS campaigns

3.2 Segmentation and evaluation of the results

The different segmentation approaches were applied to all the plots in a batch procedure without any manual interaction. The accuracy and reliability of the presented methods are evaluated in the following way: the tree positions from the segmentation are compared with reference trees if (i) the distance to the reference tree is smaller than 60% of the mean tree distance within the plot and (ii) the height difference between h_{tree} and the height of the reference tree is smaller than 15% of the top height h_{top} of the plot, where h_{top} is defined as the average height of the 100 highest trees per ha (Heurich, 2006). If a reference tree is assigned to more than one tree position, the tree position with the shortest distance to the reference tree is selected. Reference trees that are linked to one tree position are so-called 'detected trees' and reference trees without any link to a tree position are treated as 'non-detected' trees. Finally, a tree position without a link to a reference tree is referred to as a 'false positive' tree. Furthermore, the trees are subdivided into 3 layers with respect to the mean height h_{mean} of the tallest hundred trees per ha. The lower layer contains all trees below 50% of h_{mean}, the intermediate layer refers to all trees between 50% of h_{mean} and 80% of h_{mean}, and finally, the upper layer contains the rest of the trees.

3.3 Benefit of 3D segmentation

In the first instance, we will highlight how the new 3D segmentation, based on normalized cut and the stem detection method, compares to the 2D segmentation method. As described in Reitberger et al. (2008b), the normalized cut segmentation not only uses voxel coordinates but also uses features derived from the intensity and pulse width. Furthermore, tree positions calculated either from the local maxima of the segmented CHM or by the stem detection method can be utilized. These factors parameterise weighting functions, which describe the similarity between the voxels (Table 2). Therefore, we discuss the segmentation results for the data set II with respect to these options of the approach (Table 3).

The conventional watershed based segmentation ('W') leads to an overall detection rate of about 48%. As expected, the detection rate is rather poor in the lower forest layer. A combination of the watershed segmentation and the stem detection ('W+S') works successfully in the intermediate and upper layers and improves the overall detection rate by 4%.

Most notably, the 3D segmentation ('Ncut') generally increases the detection rate considerably in the lower and intermediate layers for all options. The detection rate in the upper layer does not improve, if only voxel coordinates and features are used as similarity measures.

Option:	Parameterisation of weighting function
NCut$_C$	Coordinates
NCut$_{CF}$	Coordinates, Features
NCut$_{CPm}$	Coordinates, Position of maxima from CHM
NCut$_{CPms}$	Coordinates, Positions of maxima from CHM and stem detection
NCut$_{CFPms}$	Coordinates, Features, Positions of maxima from CHM and stem detection

Table 2. Options of normalized cut segmentation

Method	Detected trees per height layer [%]				False pos. [%]
	low	intermed.	up	total	
W	5	21	77	48	4
W + S	7	27	82	52	5
NCut$_C$	18	32	77	53	6
NCut$_{CF}$	19	35	77	54	6
NCut$_{CPm}$	20	36	83	57	9
NCut$_{CPms}$	20	37	86	59	9
NCut$_{CFPms}$	21	38	87	60	9

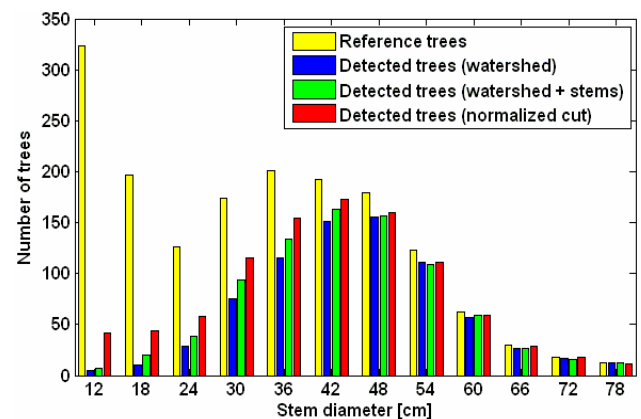Table 3. Results of segmentation methods with data set II

Figure 5. Comparison of single tree detection with data set II

If the tree positions – calculated from the local maxima of the CHM and by the stem detection – are used, the detection rate in the upper and intermediate layers is significantly improved by up to 10%. If features are used, the gain is small (by 1%) but always significant. In summary, the 3D segmentation and stem detection increase the overall detection rate by 12%. Most interestingly, the improvement is more evident in the lower and intermediate levels by about 16%. This is remarkable and shows that the new 3D segmentation technique can successfully detect smaller trees below the CHM. The high spatial point density of the full waveform data, which practically contain all relevant reflections of the laser beam, turns out as to be the key factor for segmenting in 3D, not only the dominant trees but also the dominated smaller trees in the lower and intermediate

layers. However, this increased detection rate reduces the reliability of the segmentation process by a factor of 2 in terms of false positives. Figure 5 illustrates the improvement of the detection rate graphically, but also shows that there are still many undetected smaller trees. Possible reasons, therefore, are shown in figure 6, where several smaller trees are merged to one segment. These trees remain statistically undetected since the positions and heights of the segmented trees do not correspond with the reference trees within the assumed error tolerances. However, as the figure 6 clearly shows, the 3D structure of the forest area is fully captured and separated into the dominant trees and the group of small trees of the understorey. Thus, the segments of dominant trees are mostly not affected by trees from the understorey. Subsequent analyses of tree species and timber volume will be more precise than they would be with 2D segments calculated from the watershed segmentation method.
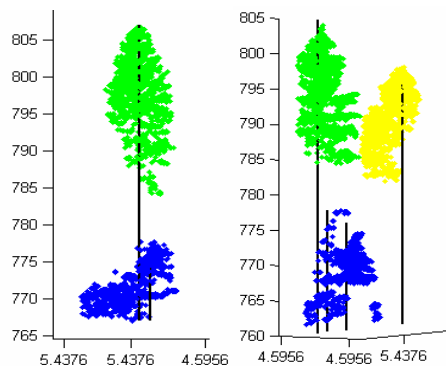

Figure 6. Two examples where several small trees are merged to one segment (blue)

3.4 Leaf-on versus leaf-off

The results given in table 3 for leaf-off conditions can also be compared with full waveform data captured in the same area and with the same point density in leaf-on condition (data set III). Table 4 shows that the watershed segmentation and stem detection do not change in all layers, both in detection rate and in reliability. Apparently, the reconstructed surface of the CHM is identical in both foliage conditions, and the crown shape of deciduous trees is well represented even in a leaf-off situation. As expected, the detection rate deteriorates in the case of the normalized cut segmentation in the lower and intermediate layer by roughly 5% due to the reduced penetration rate of the laser beam, which in turn causes a worse spatial distribution of the reflections. Finally, the number of false positives does not change significantly for the normalized cut segmentation.

Method	Detected trees per height layer [%]				False pos. [%]
	lower	intermed.	upper	total	
W	5	20	79	48	4
W + S	6	27	83	52	6
$NCut_C$	13	29	73	49	7
$NCut_{CF}$	16	29	73	50	7
$NCut_{CPm}$	15	29	82	54	9
$NCut_{CPms}$	15	31	86	57	10
$NCut_{CFPms}$	17	32	86	58	10

Table 4. Results of segmentation methods with data set III

3.5 Impact of point density

If we restrict data set III to the area E and compare it with data set IV, the impact of the nominal point density on the segmentation methods can be shown. Tables 5 and 6 demonstrate that the detection rate and false positives are practically the same for both point densities. Only the stem detection benefits from the higher point density and shows a detection rate that is 2% better than it is with lower point density. Obviously, although the number of penetrating laser beams is significantly reduced, the most relevant tree structures are still detected by reflections.

Method	Detected trees per height layer [%]				False pos. [%]
	lower	intermed.	upper	total	
W	5	20	82	55	5
W + S	6	29	87	60	7
$NCut_{CFPms}$	24	35	88	66	11

Table 5. Results of segmentation methods with data set III (only area E)

Method	Detected trees per height layer [%]				False pos. [%]
	lower	intermed.	upper	total	
W	6	21	84	57	6
W + S	7	22	86	58	7
$NCut_{CFPms}$	26	33	87	65	11

Table 6. Results of segmentation methods with data set IV (Area E)

3.6 First/Last pulse versus full waveform

Finally, we compare the segmentation methods with respect to conventional first/last pulse data (data set I; table 7) and full waveform data that have the same nominal point density (data set IV; table 6). The foliage condition is leaf-on in both cases.

Method	Detected trees per height layer [%]				False pos. [%]
	lower	intermed.	upper	total	
W	2	12	80	52	5
W + S	3	13	80	52	6
$NCut_{CPms}$	15	27	77	55	13

Table 7. Results of segmentation methods with data set I (only area E)

The total detection rate of the 2D watershed based segmentation is better by 5% for the full waveform data. The number of false positives is basically the same. The main reason for this is that the full waveform data represent the tree shape more precisely since the waveform decomposition even detects weak reflections and reflections resulting from adjacent targets. This leads to an effective point density, which is higher by a factor of 2 - 3 compared to first/last pulse data.

Contrary, first/last pulse systems ignore most of these reflections due to the inherent detection method and the dead zone of about 3 m after the first reflection. For example, figures

7a and 7b show two neighbouring spruce captured both with first/last pulse data and with full waveform data.
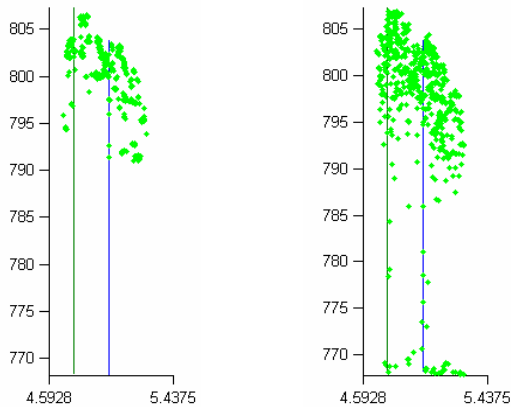

Figure 7. Neighbouring spruces captured a) with first/last pulse data and b) with full waveform data
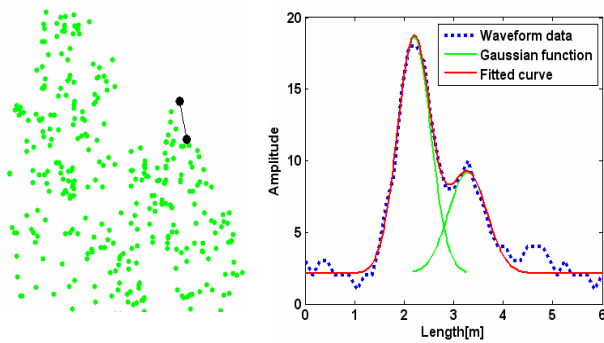

Figure 8. a) Detailed view on crown points of fig. 7b and b) waveform of the two marked points

In figure 8b, a typical waveform is depicted that results from two adjacent targets (black points in fig. 8a) with a distance of 1 m. Obviously, the tree shape is better detected by the full waveform data. If we focus on the normalized cut segmentation in tables 6 and 7 the benefit of full waveform data becomes clearer. The total detection rate amounts to 65%, which is 10% better than with first/last pulse data. Remarkable is the fact that the normalized cut segmentation increases the detection rate in the lower and intermediate layer even for the first/last pulse data.

4. DISCUSSION

The watershed segmentation method generates results that are comparable with results obtained by Heurich (2006), who obtained a detection rate of 45% in almost the same reference areas using data set I. In general, the experiments with the different data sets show that a combination of the normalized cut segmentation with the watershed segmentation and the stem detection methods always provides the best results. Using only the normalized cut segmentation with voxel coordinates improves the segmentation significantly in the lower and intermediate layers, whereas the detection rate in the upper layer is equal or even slightly worse than the detection rate of the watershed segmentation method. The implementation of the tree positions from the local CHM maxima and the stem detection improves the detection rate in the upper layer

significantly. The use of the features, intensity and pulse width, shows a small, but constant improvement.

A comparison of the different foliage conditions demonstrates a higher detection rate for the leaf-off data set mainly in the lower and intermediate layer because of the higher penetration of the deciduous trees in the leaf-off situation. Thus, the leaf-off situation seems to be the more appropriate flying time to segment trees in 3D, at least for mixed mountain forests that are scanned with a high point density. Note that the leaf-off condition is advantageous for deriving a DTM and for classifying coniferous and deciduous trees (Reitberger et al. 2008a).

The experiment with the different point densities showed that a nominal point density higher than 10 pts/m^2 does not improve the detection rate considerably. However, it remains to be seen whether a higher density would be advantageous for estimating other parameters, such as timber volume.

Finally, the experiments show that the use of full waveform data is clearly superior to first/last pulse data. All segmentation approaches shown in this paper work better with full waveform data. Most notably, only the normalized cut segmentation can take advantage of the high spatial point density that the full waveform technique provides. In summary, the significant improvement of the detection rate – especially apparent in the lower and intermediate layers – is influenced both by the full waveform data and the new normalized cut segmentation.

5. CONCLUSIONS

We have shown in this paper how several segmentation methods work with conventional first/last pulse data and full waveform data. The combination of a new normalized cut segmentation with the tree positions derived with watershed segmentation or stem detection methods leads to a significant improvement in the detection rate, especially in the case of full waveform data.

LITERATURE

Brandtberg, T., 2007. Classifying individual tree species under leaf-off and leaf-on conditions using airborne lidar. *ISPRS Journal of Photogrammetry and Remote Sensing*, 61, pp. 325 – 340.

Heurich, M., 2006. Evaluierung und Entwicklung von Methoden zur automatisierten Erfassung von Waldstrukturen aus Daten flugzeuggetragener Fernerkundungssensoren. Forstlicher Forschungsbericht München, Nr. 202, ISBN 3-933506-33-6. http://meadiatum2/ub.tum.de/. (Accessed February 18, 2007).

Hyyppä, J., Kelle, O., Lehikoinen, M., Inkinen, M., 2001. A segmentation-based method to retrieve stem volume estimates from 3-D tree height models produced by laser scanners. *IEEE Transactions on Geoscience and remote Sensing,* 39:969-975.

Jutzi, B., Stilla, U., 2005. Waveform processing of laser pulses for reconstruction of surfaces in urban areas. In: Moeller M, Wentz E (eds) 3th International Symposium: Remote sensing and data fusion on urban areas, URBAN 2005. International

Archives of Photogrammetry and Remote Sensing. Vol 36, Part 8 W27.

Jutzi, B., Stilla, U., 2006. Range determination with waveform recording laser systems using a Wiener Filter. *ISPRS Journal of Photogrammetry and Remote Sensing*, 61, pp. 95–107.

Kirchhof, M., Jutzi, B., Stilla, U., 2008. Iterative processing of laserscanning data by full waveform analysis. *ISPRS Journal of Photogrammetry and Remote Sensing*, 63, pp. 99–114.

Reitberger, J., Krzystek, P., Stilla, U., 2007. Combined tree segmentation and stem detection using full waveform LIDAR data. *IAPRS* Volume XXXVI, PART 3/W52, 12 – 14th September 2007, Espoo, pp. 332 – 337.

Reitberger, J., Krzystek, P., Stilla, U., 2008a. Analysis of full waveform LIDAR data for the classification of deciduous and coniferous trees. *International Journal of Remote Sensing*. Vol. 29, No. 5, March 2008 , pp. 1407 – 1431.

Reitberger, J., Schnörr, Cl., Krzystek, P., Stilla U., 2008b. 3D Segmentation of Full Waveform LIDAR data for Single Tree Detection using Normalized Cut. *ISPRS 21th Congress*, Peking, China, 3 – 11th July 2008.

Shi, J., Malik, J., 2000. Normalized cuts and image segmentation. *IEEE Transactions on Pattern Analysis and Machine Intelligence*, 22, pp. 888-905.

Solberg, S., Naesset, E., Bollandsas, O. M., 2006. Single Tree Segmentation Using Airborne Laser Scanner Data in a Structurally Heterogeneous Spruce Forest. *Photogrammetric Engineering & Remote Sensing,* Vol. 72, No. 12, December 2006, pp. 1369-1378.

Wagner, W., Ullrich, A., Ducic, V., Melzer, T., Studnicka, N., 2006. Gaussian decomposition and calibration of a novel small-footprint full-waveform digitising airborne laser scanner. *ISPRS Journal of Photogrammetry and Remote Sensing*, 60, pp. 100 – 112.